



Magnesium-Rich Nanometric Layer in the Skeleton of *Pocillopora damicornis* With Possible Involvement in Fibrous Aragonite Deposition

Orr H. Shapiro^{1,2*}, Elena Kartvelishvily^{3†}, Esti Kramarsky-Winter² and Assaf Vardi^{2*}

OPEN ACCESS

Edited by:

Jessica Carilli,
University of Massachusetts Boston,
United States

Reviewed by:

Aldo Cróquer,
Simón Bolívar University, Venezuela
Jarosław Stolarski,
Institute of Paleobiology (PAN), Poland

*Correspondence:

Orr H. Shapiro
orr@agri.gov.il
Assaf Vardi
assaf.vardi@weizmann.ac.il

†These authors have contributed
equally to this work.

Specialty section:

This article was submitted to
Coral Reef Research,
a section of the journal
Frontiers in Marine Science

Received: 24 February 2018

Accepted: 26 June 2018

Published: 17 July 2018

Citation:

Shapiro OH, Kartvelishvily E,
Kramarsky-Winter E and Vardi A
(2018) Magnesium-Rich Nanometric
Layer in the Skeleton of *Pocillopora*
damicornis With Possible Involvement
in Fibrous Aragonite Deposition.
Front. Mar. Sci. 5:246.
doi: 10.3389/fmars.2018.00246

¹ Agricultural Research Organization, Department of Food Quality and Safety, Volcani Center, Rishon LeZion, Israel, ² Department of Plant and Environmental Sciences, Weizmann Institute of Science, Rehovot, Israel, ³ Unit of Electron Microscopy, Department of Chemical Research Support, Weizmann Institute of Science, Rehovot, Israel

The complex structures and morphologies of coral skeletons make it difficult to study the construction of individual skeleton components. This is especially true regarding micro-structures deposited during different stages of skeletogenesis. As such structures serve as the basis for subsequent skeleton development, they are often obscured by additional skeletal deposition and growth. Recently we described a new model system, coral-on-a-chip, for studying coral biology, and skeletogenesis. This system utilizes micropropagates of the Indo-Pacific coral *Pocillopora damicornis* maintained within a microfluidic environment, allowing us to follow early stages of skeletogenesis over time and under controlled environmental conditions. Our findings reveal that, following settlement onto glass slides, the micropropagates initially form a thin, almost two dimensional skeleton, which subsequently develops into a robust three-dimensional form with features resembling those of the mother colony. Studying the early stages of skeleton accretion in our micropropagates using high-resolution scanning electron microscopy and Energy Dispersive X-ray Spectroscopy (EDS) revealed a magnesium-rich layer deposited directly on the glass surface. This layer, which has a typical Mg/Ca ratio of 1.43 ± 0.78 , forms a dense lattice with a typical pore size of 100 nm. Microscopic observations indicate that this lattice serves as the basis for subsequent growth of fibrous aragonite. Examination of the underside of a skeleton from a small *P. damicornis* colony growing on a glass surface revealed a similar high-magnesium lattice at the interface between the glass and aragonitic skeleton in association with fibrous aragonite deposition. These observations suggest a role for this magnesium-rich lattice in the deposition of the fibrous aragonite forming the bulk of the coral skeleton.

Keywords: coral calcification, coral skeletogenesis, microscale skeletal features, coral micropropagate, coral on a chip, brucite, magnesium compounds, marine biology

INTRODUCTION

Despite over a century of scientific research, many of the microscale mechanisms underlying coral calcification remain elusive. Based on our current understanding, coral skeletogenesis is thought to consist of two distinct phases, an organic-rich mineral phase, described by various researchers as centers of calcification (CoC) (Cuif and Dauphin, 1998), early mineralizing zone (EMZ) (Cuif et al., 2003), or rapid accretion deposits (RAD) (Brahmi et al., 2010), and a phase consisting of layered fibrous aragonite, termed thickening deposits (Stolarski, 2003). The two main models for coral calcification posit that these phases are either deposited simultaneously, but differ in growth dynamics (Stolarski, 2003; Brahmi et al., 2012; Domart-Coulon et al., 2014), or follow a cyclic, two-step process where the CoC is deposited first, followed by deposition of fibrous aragonite perpendicular to the surface of the CoC (Cuif and Dauphin, 2005; Von Euw et al., 2017).

The deposition of the aragonitic skeleton, and the different structures that characterize different coral species (Cuif and Dauphin, 1998; Stolarski, 2003), is thought to be governed by two main biological processes. On the one hand, corals actively modify the pH and mineral composition of water at the calcification site, producing a high CaCO_3 saturation state favoring aragonite precipitation (Allison et al., 2014). On the other hand, a skeletal organic matrix, consisting of acid-rich proteins, serves as a template for aragonite nucleation and subsequent skeletal growth (Mass et al., 2013; Von Euw et al., 2017). Much research has been dedicated to the mineral composition of specific compartments of coral skeletons (Cuif and Dauphin, 1998; Meibom et al., 2004; Brahmi et al., 2010; Gutner-Hoch et al., 2016; Giri et al., 2017). In addition to calcium, two of the most abundant mineral components of coral skeletons are strontium (Sr) and magnesium (Mg). (Leclerc et al., 2014; Giri et al., 2017). While Sr concentrations are relatively stable throughout the skeleton, Mg concentrations show a highly uneven distribution, with significantly elevated levels in the CoC relative to those found in fibrous aragonite (Meibom et al., 2004, 2007; Brahmi et al., 2010). Moreover, Mg banding is repeatedly observed within the fibrous skeleton compartment of multiple coral species, with a typical band-width of approximately $5 \mu\text{m}$ (Meibom et al., 2004, 2007, 2008). Interestingly, these structures appear to be specifically associated with zooxanthellate corals, and may correspond to diurnal light/dark cycles (Frankowiak et al., 2016). These findings suggest a strong biological control over the magnesium content of specific components within the coral skeleton, indicating an important role for this ion in coral skeletogenesis. While this “vital effect” (*sensu* Meibom et al., 2006) is likely to be associated with specific Mg-rich microscale structures, to date no such structures have been described.

One reason for the difficulty in observing and studying specific microscale stages in coral skeletogenesis is that continuous skeleton formation masks intermediate stages, making them difficult to characterize. Recently we reported the development of a new coral model system, the “Coral on a Chip” (Shapiro et al., 2016), which utilizes coral micropropagates, derived from an adult *P. damicornis* colony and settled on clean glass

slides, for studying microscale calcification and other coral biology processes. Here we report results from scanning electron microscopy of the early stages of calcification by these initially skeleton-free micropropagates. We consistently observed an Mg-rich microstructure deposited by these micropropagates at the glass-skeleton interface, that appears to be distinct from the overlying aragonitic skeleton. We further demonstrate close association of fibrous aragonite growth with these structures. We also show similar structures at the glass-skeleton interface in lateral growth of small *P. damicornis* colonies, again in close association with fibrous aragonite. These observations suggest a possible role for the observed Mg-rich lattice in the deposition of fibrous thickening deposits in *P. damicornis*.

METHODS

Coral Growth Conditions

Small colonies of the coral *Pocillopora damicornis* were collected by permit from the reef opposite the Inter-University institute in Eilat, Israel and were maintained in a dedicated aquarium system under 24°C , at a light intensity of $200 \mu\text{mol photons m}^{-2} \text{s}^{-1}$, and under a 12 h light-dark cycle. Artificial seawater (39 ppt) was prepared by dissolving Reef Salts (Aqua Medic GMBH, Germany) in deionized water.

Coral micropropagates were generated by “polyp bail-out,” as described in Shapiro et al. (2016). Shortly, micropropagation was induced by exposing coral fragments to a gradual increase in salinity up to 56 ppt. Released micropropagates were collected and transferred to microwells constructed on clean glass slides (Sail Brand, China). Slides with micropropagates were incubated in especially designed race-way system under ambient salinity; 25°C ; 1 cm s^{-1} flow; $120 \mu\text{mol photons m}^{-2} \text{s}^{-1}$ light; 12 h day/night cycle and checked for settlement over the next 48 h.

Light Microscopy

The explant-containing channel was mounted on a motorized XY stage (Prior Scientific, MA, USA) with a temperature-controlled inset (LCI, Korea). The microwell was sealed and care was taken to avoid trapping of bubbles that may interfere with transmitted light microscopy. An inlet tube connected to one end of the channel draws water from a reservoir containing the incoming water and an outlet is connected at the other end to a syringe pump (New Era Pump Systems, NY, USA) set to withdraw mode. This ensures a negative pressure in the channel to avoid leakage. Flow rate was set to 1 ml/h for all experiments reported here. All light microscopy imaging was performed using an Olympus IX81 microscope equipped with a Lumen 200PRO illumination system (Prior Scientific, MA, USA).

Calcein Staining

Calcein staining was performed by introducing $20 \mu\text{M}$ calcein solution in ASW into the chamber inlet for a period of 1 h. Inlet was then changed back to ASW and free calcein was washed out. Tissue, organic residues and unincorporated calcein were removed by washing the chamber with 1% NaOCl in distilled water for a period of 1 h, followed by 10 min of filter-sterilized

tap water. Calcein was observed by epifluorescence microscopy [Ex:490-Em:535/50 nm (Chroma, USA)].

Scanning Electron Microscopy

Settled explants were washed in 1% sodium hypochlorite in distilled water for 1 h to remove tissues and organic residues. The glass slide was cut around the exposed skeleton using a glass cutter and the skeleton dehydrated by immersion in 100% ethanol. Prior to imaging, the skeletons were dried under vacuum and carbon coated. Imaging and Energy Dispersive Spectroscopy (EDS) measurements were performed using a Carl Zeiss Ultra 55 scanning electron microscope. Calibration was performed against Cu and Ti standards, and Mg/Ca ratio was calculated by dividing the appropriate molar concentration values returned by the EDS measurement.

Lateral Skeleton Preparation

Lateral skeleton preparation (LSP) in *P. damicornis* colonies was obtained by gluing 1 cm nubbins to clean glass slides using Loctite superglue (Raz-Bahat et al., 2006). Nubbins were kept in the aquarium until the formation of a thin layer of tissue and skeleton was observed on the glass around the base of the nubbin. This layer was carefully detached from the glass slide using a clean scalpel. The detached skeleton was prepared for SEM as described above and attached to an aluminum EM stub using carbon tape, with bottom surface facing up. Skeleton was vacuum dried and carbon coated and SEM carried as described above.

Skeleton dissolution by egtazic acid (EGTA) was performed on small section of LSP-covered glass. Tissue and organic material were first removed by immersion in 1% NaOCl for 1 h, followed by quick rinse in filter-sterilized tap water and dehydration in 100% ethanol. Glass and exposed skeleton were then immersed in 5 ml of 5 mM EGTA in distilled water for 1 h at room temperature. The resulting preparation was again dehydrated in 100% ethanol, vacuum dried, and carbon coated prior to SEM imaging.

RESULTS

De-Novo Skeletogenesis by *Pocillopora damicornis* Micropropagates

Initial skeleton formation in settled micropropagates is readily observed 24 h following settlement. Polarizing crystals are evident throughout the area covered by the settled polyps' soft tissues, accumulating most rapidly at the polyp's periphery (Figures 1A,B). In settled micropropagates a raised calyx wall (part of the polyp "cup") is typically formed within 5 days of settlement (Figure 1B). The area forming the calyx basal plate is gradually filled-in, concomitantly with growth of the calyx wall. Regularly-spaced spinules (needle-like skeletal protrusions) and septa (skeletal features partitioning the skeletal cup) subsequently develop, completing the calyx structure.

Calcein staining of settled polyps indicated preferential labeling of protruding structures, including septa, spinules, and calyx wall, while little or no labeling of basal plate structures was observed (Figure 1C). Scanning electron microscopy (SEM) revealed clear differences between these differentially-labeled

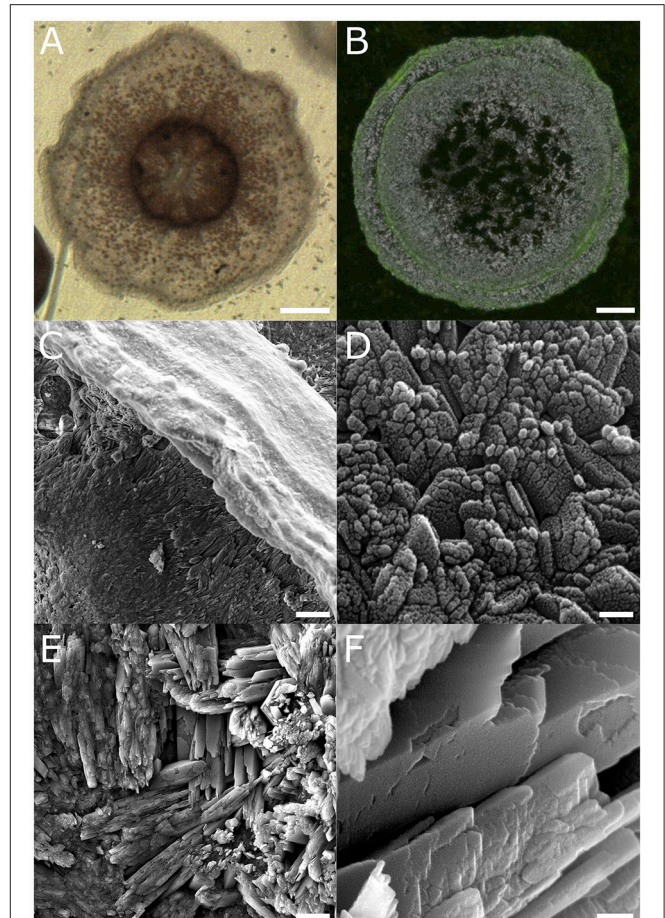


FIGURE 1 | Two distinct phases observed in the skeleton of *P. damicornis* micropropagates. **(A)** Micropropagate from a *P. damicornis* 24 h following settlement. Polyp mouth is seen in the center surrounded by septa. Brown dots are individual zooxanthellae cells. Scale –250 μm . **(B)** Skeleton of a *P. damicornis* micropropagate 5 days after settlement, following calcein staining and bleach treatment. Visualization by a combination of polarized light microscopy (gray scale) and epifluorescence (green). Green fluorescence, denoting calcein incorporation, was largely restricted to protruding structures (such as the calyx wall), with little or no incorporation observed within the basal plate area. Scale –100 μm . **(C–F)** High resolution SEM showing the skeleton of a micropropagate 6 weeks from settlement. **(C)** Low magnification view of the calyx wall, corresponding to the area labeled with calcein in **(B)** shows a characteristically smooth surface. **(D)** High magnification of the top of the calyx wall shown in **(C)** reveals nm-scale granulation. **(E)** Large crystals of fibrous aragonite growing at various orientations compose the calyx basal plate. **(F)** High magnification of the fibrous aragonite in **(D)** reveals the smooth surface of individual fibers, suggesting a different calcification process from the calyx wall and similar protruding structures. Scale bars: **(C,E)**–10 μm , **(D,F)**–0.1 μm .

structures. While protruding structures were composed of nanometer-sized granules arranged in rhomboid-like structures (Figures 1C,D), the fibrous crystals forming the calyx basal plate appeared smooth with no granulation (Figures 1E,F).

A Magnesium Rich Lattice Is Deposited Prior to Base-Plate Calcification

The newly-deposited basal plate of settled micropropagates is formed by deposition of fibrous aragonite crystals at multiple

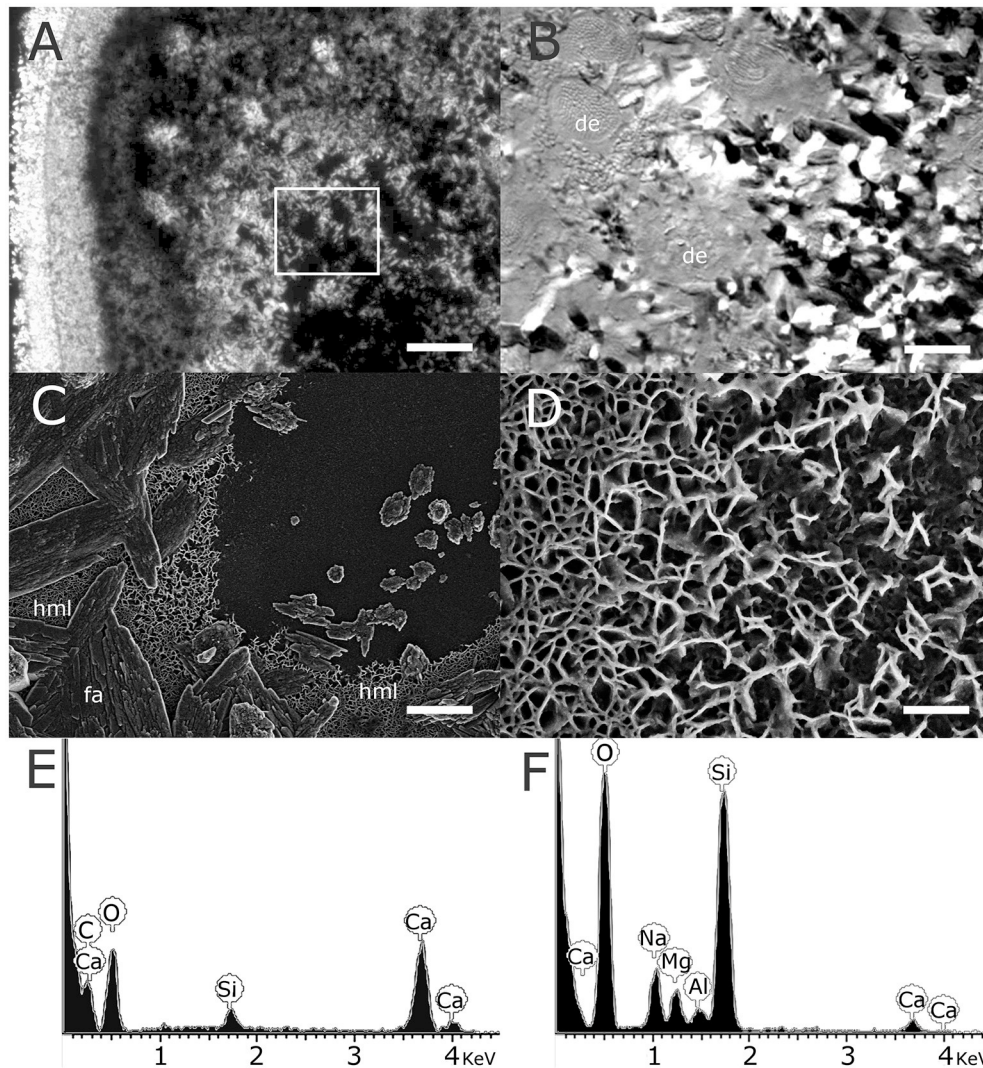


FIGURE 2 | High magnesium lattice deposited by the coral precedes the precipitation of fibrous aragonite. **(A)** Polarized light microscopy showing the basal plate of a live micropropagate 2 weeks following settlement, with clay edge to the left. Scale $-100\ \mu\text{m}$. **(B)** Differential interference contrast microscopy showing high magnification of the region denoted by the white rectangle in **(A)**. Gaps between the aragonite fibers forming the basal plate where often associated with round or oval desmoidal cells (de) with a typical diameter of $20\ \mu\text{m}$ attaching the coral tissue to the glass substrate. Scale $-20\ \mu\text{m}$. **(C)** High resolution SEM showing details of the basal plate of a micropropagate, showing fibrous aragonite (fa) overlaying a high magnesium lattice (hml) deposited on the glass substrate. Scale $-3\ \mu\text{m}$. **(D)** High magnification SEM revealing a nanometer scale lamellar structure. Scale $-0.5\ \mu\text{m}$. **(E, F)**—EDS analysis of the fibrous aragonite and lattice structures seen in **(C)**, showing low calcium and high magnesium levels in the hml (sodium and silica signals are likely derived from the glass substrate).

locations, ultimately fusing to form the continuous basal plate structure. Large gaps between these growing crystals are easily observed by polarized light microscopy, particularly at early stages of calcification (**Figure 2A**). DIC microscopy revealed that these gaps are often associated with desmocytes, cells anchoring the coral tissue to the skeleton or the substrate (**Figure 2B**). High magnification SEM imaging of these gaps revealed an irregular lattice-like structure, with a typical spacing of $100\ \text{nm}$, deposited directly on the glass substrate and preceding the formation of aragonite crystals (**Figures 2C, D**). Energy Dispersive X-ray Spectroscopy (EDS) analysis of this structure revealed high molar Mg/Ca ratios, on the order of 1:1–3:1 (**Figure 2E**, **Table 1**),

making it distinctly different from the overlying calcium carbonate crystals in both structure and composition (**Figure 2F**, **Table 1**). No similar structure was observed on the glass surface beyond the polyp's perimeter.

We further observed circular patches, approximately $20\ \mu\text{m}$ in diameter, where this lattice structure was less dense or completely absent (**Figures 3A–D**). The size and shape of these patches are consistent with desmoidal processes anchoring the coral polyp to the glass surface (**Figure 2B**). Interestingly, calcium carbonate deposition within these circular patches was markedly different from crystal deposited on the surrounding lattice. Elongated, ordered aragonite crystal were found growing on top of the Mg

TABLE 1 | Mg/Ca ratios at different sites examined during this study.

Sample	Location	Number of readings	Mg/Ca		
			Range	Average	SD
Micropropagate	Lattice	15	0.7–3.2	1.43	0.78
	Aragonite (small)	5	0.1–0.4	0.24	0.11
	Aragonite (large)	5	0–0.05	0.03	0.02
	Glass	3	0.8–0.9	0.87	0.06
LSP underside	High Mg patch	4	0.1–0.2	0.15	0.06
	RFA center	4	0.2–1.2	0.65	0.41
	RFA Fibers	5	0.005–0.08	0.02	0.03

LSP, lateral skeleton preparation; RFA, radiating fibrous aragonite.

rich lattice, while calcium carbonate deposited on the exposed glass surface had an amorphous appearance (Figure 3F).

Evidence Forsimilar Mg-Rich Lattice Is in a *P. damicornis* Colony

To ascertain that micropropagate skeletogenesis is comparable to that of colonies, we compared our results to *P. damicornis* skeleton produced by LSP. A lamellar structure similar to that found in micropropagates was found at the interface between LSP-produced skeleton and the glass surface on which it was grown (Figures 4A–D). Associated with this structure we repeatedly observed small circular features (SCF), with a typical diameter of 2 μ m (Figures 4A–D). Following EGTA treatment of LSP attached to the glass surface, both the lamellar structure and SCFs were exposed, consistent with a Mg-rich composition. EDS analysis of these structures revealed a Mg/Ca ratio of approximately 0.25 (Figure 4E). EDS analysis of lamellar structures and SCF following EGTA treatment revealed trace levels of Mg, with Ca levels below detection limit.

Further analysis of the underside of LSP from the same *P. damicornis* colony revealed that aggregations of SCF are associated with areas of high-Mg content (Figures 4E,G). These areas were surrounded by patches of radial fibrous aragonite (RFA) (Figures 4E,F). In the center of these RFA patches we often observed a circular, aragonite-free structure a few micrometers in diameter (Figure 4F). EDS measurements indicated elevated Mg/Ca ratios within these structures compared to surrounding aragonite (Figures 4G,H, Table 1).

DISCUSSION

Despite over a century of research on coral skeletogenesis, much remains to be learned about the microscale processes governing this globally important process. Coral calcification is known to depend on multiple parameters including pH, temperature, nutrient and light availability, and others (Reynaud et al., 2007; Kramarsky-Winter et al., 2009; Venn et al., 2011, 2013; Kvitt et al., 2015). However, the mechanisms linking such environmental parameters with the microscale processes shaping the coral skeleton remain elusive. In recent years, much effort has been dedicated to the elucidation of these microscale processes,

assisted by advances in microscopy and molecular biological tools (Meibom et al., 2006; Raz-Bahat et al., 2006; Venn et al., 2011; Mass et al., 2017; Von Euw et al., 2017). Such studies are critical for our ability to understand and predict the effects of environmental changes due to natural and anthropogenic influences on the future of coral reefs.

Here we report for the first time the presence of a nanometer-thick lattice deposited during skeletogenesis of the Indo-Pacific coral *P. damicornis*. This lattice was first observed while studying the skeletons of micropropagated *P. damicornis* polyps settled on clean glass slides. Differential incorporation of calcein into different skeletal compartments, demonstrated previously (Shapiro et al., 2016), is confirmed in the present study (Figure 1B). We further show that these different skeletal compartments consist of two distinct aragonite forms. One form, found in protruding skeletal features such as septa, spinules, and calyx edge, is granulated, composed of spherical particles of approximately 20–40 nm (Figures 1C,D), similar to previous observation in other coral species (e.g., Cuif and Dauphin, 2005). In contrast, crystals resembling fibrous aragonite are smooth, with no apparent granulation (Figures 1E,F), suggesting a different calcification process.

In close association with the fibrous aragonite composing the polyps' basal plate we consistently observed a nanometer-scale lattice of irregular spacing, clearly distinguished from other layers of the newly-formed skeleton of settled micropropagates (Figures 2C,D). Importantly, this layer was observed only within the perimeter of area covered by the coral tissue, indicating that its deposition is driven, and possibly controlled, by the coral animal. Furthermore, the repeated observation of lattice-devoid, or partially filled, circular patches (Figures 3A–D) in this layer, suggests that lattice deposition occurs around desmocytes (Figure 2B), specialized cells anchoring the coral tissue to the skeleton or the substrate (here the glass slide).

Perhaps the most striking feature of the lattice described here is its exceptionally high magnesium to calcium ratio, on the order of 1–3 mol Mg/mol Ca. Whole-skeleton measurements reported from different coral species consistently yielded Mg/Ca ratios on the order of 5 mmol/mol (Leclerc et al., 2014; Giri et al., 2017). Precise values vary between specific compartments within the skeleton, from 2 to 4 mmol/mol in fibrous aragonite to 10–15 mmol/mol in CoC (Cuif and Dauphin, 1998; Meibom et al., 2004, 2008; Gagnon et al., 2007; Brahmi et al., 2012). The observed Mg/Ca ratios measured in the lattice we describe are thus nearly a thousand-fold higher than most coral-associated skeletal structure reported to-date.

The only previous reports of similar Mg/Ca ratios in any component of a coral skeleton are from deposits of brucite [Mg(OH)₂], found in skeletons deposited by several coral species including *Pocillopora*, *Acropora*, *Porites* (Nodthdruff et al., 2005), and *Monstastrea* (Buster and Holmes, 2006). These deposits had a similar EDS signature to that of the lattice observed here, and some of them appear very similar in SEM images, suggesting a similar composition for the lattice we describe here. However, both these reports suggest brucite deposits to be associated with, and possibly mediated by, endolithic algal or microbial mats. Our observations appear to be inconsistent with this explanation, as

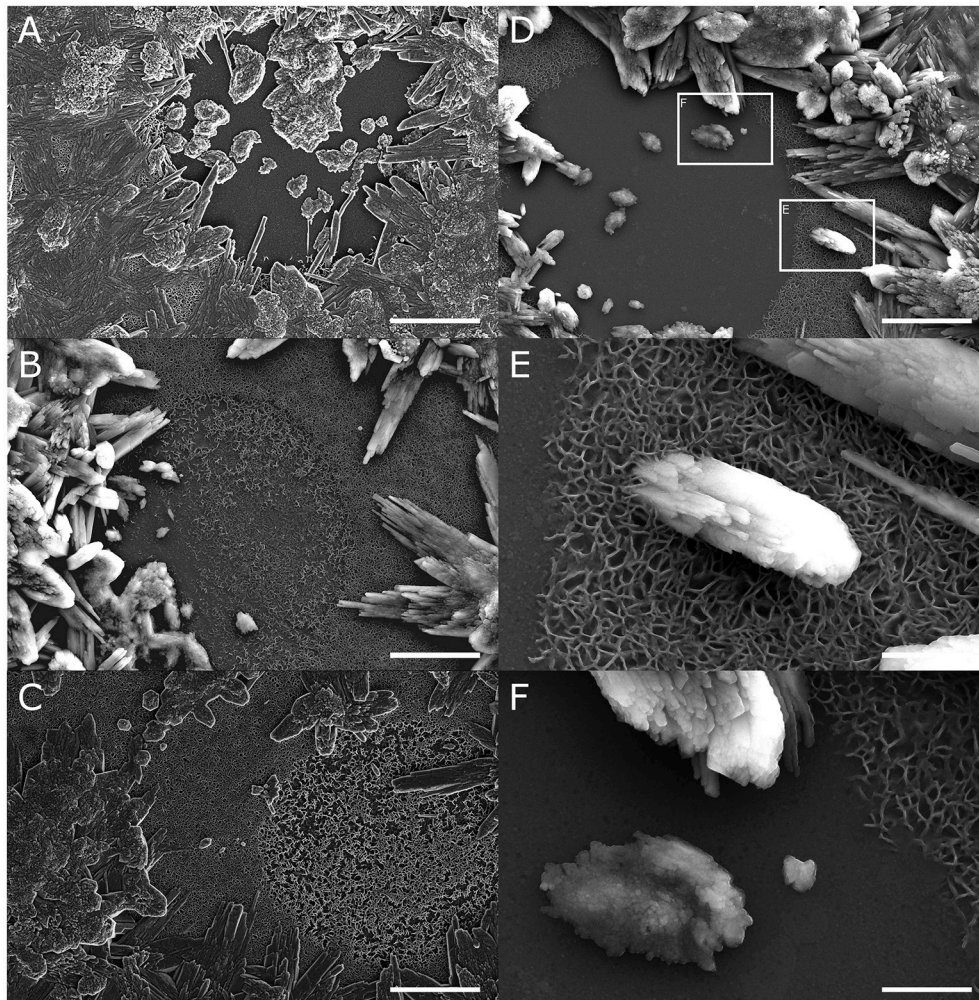


FIGURE 3 | The high magnesium lattice (hml) may direct growth of fibrous aragonite. **(A–D)** Round or oval patches, approximately 20 μm in diameter, are frequently observed within the hml, where the structure is either completely absent or appears less dense. Fibrous aragonite is deposited on the hml around these patches but not within them. Scale bars –5 μm . **(E,F)** High magnification of CaCO_3 deposits show a distinct difference between the fibrous aragonite deposited on top of the hml **(E)** and amorphous structures deposited within patches where hml is missing **(F)**. Scale bars –1 μm .

we did not observe any structures resembling algae or bacteria in association with the Mg-rich lattice. Moreover, no algae (other than zooxanthellae), and very few bacteria, were revealed by light and fluorescent microscopy of the glass-tissue interface, afforded by the unique coral preparation we utilized in our experiments. An artifact due to the application of bleach during the cleaning process, also suggested as a possible source for brucite (Buster and Holmes, 2006), can also be ruled here as the lattice was invariably observed between the aragonitic skeleton and the glass, rather than on top of the aragonite surface exposed to the bleach. We thus conclude that the lattice we observe is most likely produced by the coral itself, and not some associated microbial life form.

The observation of the Mg-rich lattice was made possible by the unique features of our micropropagate-based platform, which allows us to microscopically observe discrete stages within the

calcification process. Our findings clearly demonstrate that, in our micropropagates, the observed lattice is deposited directly on the glass surface, prior to the deposition the first layer of fibrous aragonite. Moreover, fibrous aragonite crystals are formed in direct contact with this lattice (**Figure 3E**). Interestingly, calcium deposits within circular patches devoid of this lattice consistently appeared less ordered, resembling amorphous calcium carbonate (**Figure 3F**). This suggests a role for the observed Mg-rich lattice in directing aragonite deposition and growth.

The presence of a similar lattice on the underside of *P. damicornis* colonies growing on a glass surface rules out the possibility that this lattice is a peculiarity of micropropagate calcification. Mg-rich structures were localized to two distinct features of the underside of *P. damicornis* LSP. One such structure is associated with clusters of SCF, 2 μm in diameter. We propose that each SCF is formed by a desmoidal process

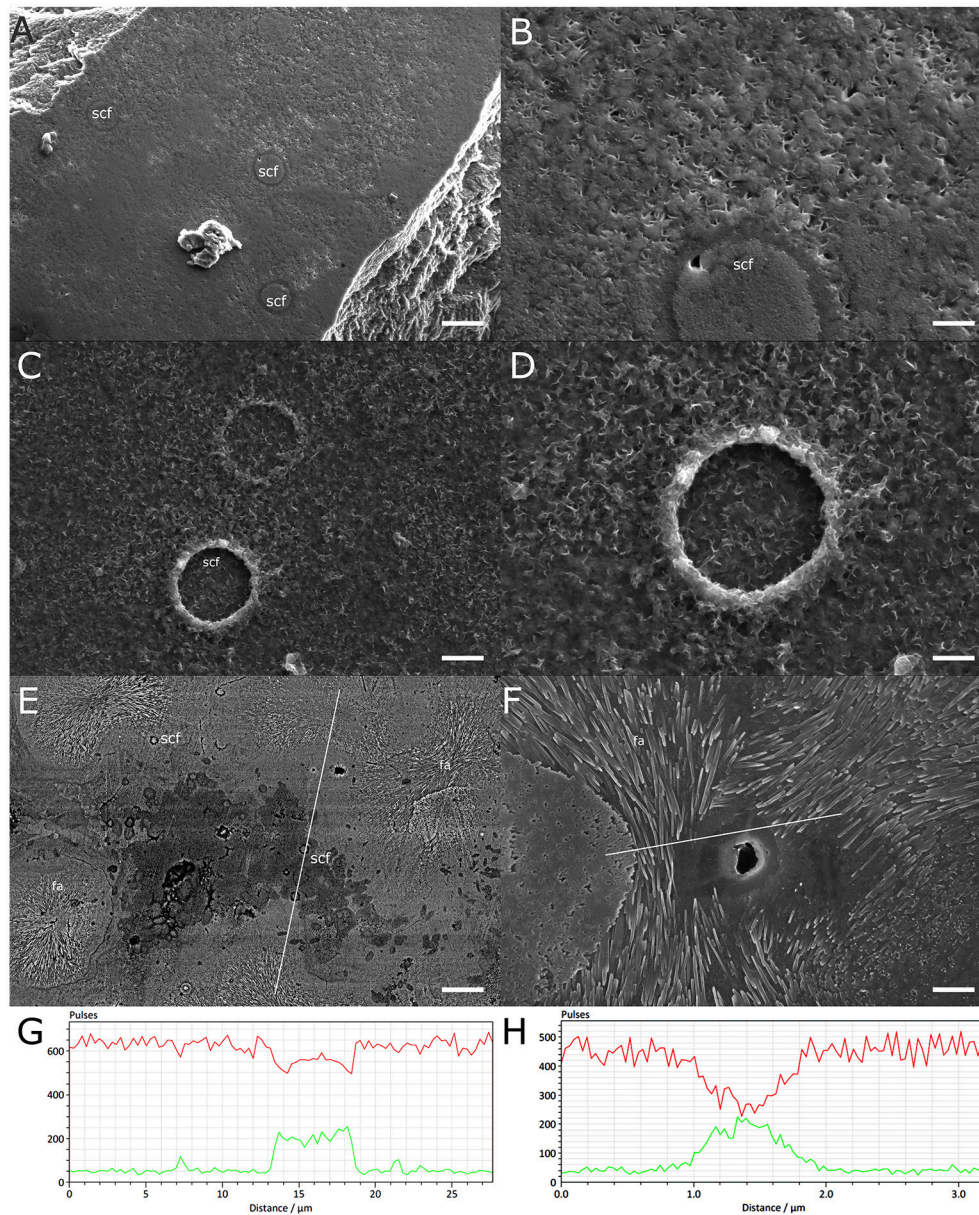


FIGURE 4 | High magnesium structures at the base of a *P. damicornis* colony grown on a glass surface. **(A)** Underside of the skeleton of a small colony, showing small circular features (scf) embedded in the skeletal matrix. Scale—2.5 μm . **(B)** High magnification of the surface shown in **(A)**, showing an scf surrounded by a lattice similar to hml observed in micropropagates. Scale—0.5 μm . **(C,D)** Residues left on the glass surface following dissolution of the skeleton of a small *P. damicornis* colony by EGTA, preferentially chelating Ca over Mg. Scf structures are embedded in the hml and appear slightly raised. Scale—1, 0.5 μm for **(C,D)**, respectively. **(E)** Backscatter analysis of the underside of a small colony, with high Mg areas appearing darker. Multiple scfs are seen within the high Mg patch or surrounding it. Patches of radially growing fibrous aragonite (fa) surround the high Mg patch. White line marks the path of the EDS transect shown in **(G)**. Scale—8 μm . **(F)** A patch of radially growing fibrous aragonite surrounding a central pit. White line marks the path of the EDS transect shown in **(H)**. Scale—2.5 μm . **(G,H)** Changes in Ca (red) and Mg (green) levels along EDS transects from **(E,F)**, respectively. High Mg/Ca ratios are evident within the dark patch in **(E)** and next to the pit in **(F)**.

made up of several adjacent plaques (*sensu* Muscatine et al., 1997). Thus, SCF clusters, like the larger circular features observed in micropropagates, are formed by desmocytes anchoring the soft tissue to the glass substrate. The difference in appearance of these processes between micropropagates and LSP preparation may be explained by the disturbance

experienced by the coral tissue following the micropropagation and resettlement process. A 2nd structure, found surrounding the observed SCF clusters, is directly associated with growth of fibrous aragonite, further supporting the involvement of the observed high-Mg lattice in fibrous aragonite deposition.

Fibrous aragonite is a major component the skeletal structure of modern scleractinian corals (Stolarski, 2003; Cuif and Dauphin, 2005; Gutner-Hoch et al., 2016). Several models for coral skeletogenesis suggested to-date propose fibrous aragonite to be a secondary step of skeleton growth, preceded by the formation of centers of calcification (Bryan and Hill, 1941; Cuif et al., 2003; Von Euw et al., 2017). In contrast to these models, but possibly in agreement with the simultaneous deposition model proposed by Stolarski (2003), we observe fibrous aragonite in the skeleton of *P. damicornis* growing on top of a Mg-rich lattice deposited directly on a glass substrate in both micropropagates and colonies. Interestingly, following EGTA treatment, the SCF structures appeared intact while the Mg content was hardly distinguishable from that of the glass substrate. This may indicate that the observed lamellar structure is an organic matrix with high affinity for Mg, as proposed previously for high-Mg bands in fibrous aragonite (Frankowiak et al., 2016).

Although magnesium is known to play a pivotal role in calcification processes, its role in shaping the complex coral skeletal structure still remains a central question in the field of coral skeletogenesis. Multiple studies have demonstrated that centers of calcification are particularly rich in Mg (Cuif and Dauphin, 1998, 2005; Meibom et al., 2004, 2007, 2008; Holcomb et al., 2009). This has been explained by a possible role of Mg in stabilizing the amorphous calcium carbonate nanoparticles serving as the building blocks of CoC (Mass et al., 2017; Von Euw et al., 2017). This is further supported by reports that corals grown in seawater with low Mg/Ca ratios produce skeletons with a high proportion of calcite (Higuchi et al., 2014), indicating an important role of Mg in stabilizing the prevalent aragonitic form of modern-day corals. While Mg content in fibrous aragonite is distinctly lower than in the CoC, a clear banding pattern in Mg/Ca ratio in these structures has been demonstrated by microscale measurement in multiple coral species (Meibom et al., 2004, 2007, 2008; Gagnon et al., 2007; Frankowiak et al., 2016),

suggesting Mg is concentrated at the interfaces between adjacent fibrous aragonite layers (Frankowiak et al., 2016).

To conclude, we show that a Mg-rich lamellar structure is deposited by *P. damicornis* during skeletogenesis, possibly in association with desmoidal processes. We further show that growth of fibrous aragonite is closely associated with these lamellar structures and may even be directed by them. Further studies are required to establish role of these Mg-rich structures in skeletogenesis of *P. damicornis*, and possibly in other coral species. Understanding the role of these structures may be of particular interest in the context of ocean acidification, which affects the aragonite saturation state of seawater and may thus interfere with coral calcification. Our results further demonstrate the potential of coral micropropagates for studying skeletogenesis, providing a new window into the microscale processes governing coral calcification processes.

AUTHOR CONTRIBUTIONS

OS and EK-W developed the coral micropropagation system. OS, EK, and EK-W performed electron microscopy and EDS analysis. AV directed the work and participated in experimental design. All authors contributed to manuscript writing.

FUNDING

This work was supported by the Human Frontiers in Science Program award #RGY0089, the Weizmann—EPFL Collaboration Program (grant number: 721236), and the Angel Faivovich Foundation for Ecological research.

ACKNOWLEDGMENTS

The authors thank Assaf Gavish for help with coral collection and maintenance. Dr. Assaf Gal and Prof. Jonathan Erez are acknowledged for useful discussions.

REFERENCES

- Allison, N., Cohen, I., Finch, A.A., Erez, J., and Tudhope, A.W. (2014). Corals concentrate dissolved inorganic carbon to facilitate calcification. *Nat. Commun.* 5:5741. doi: 10.1038/ncomms6741
- Brahmi, C., Kopp, C., Domart-Coulon, I., Stolarski, J., and Meibom, A. (2012). Skeletal growth dynamics linked to trace-element composition in the scleractinian coral *Pocillopora damicornis*. *Geochim. Cosmochim. Acta* 99, 146–158. doi: 10.1016/j.gca.2012.09.031
- Brahmi, C., Meibom, A., Smith, D.C., Stolarski, J., Auzoux-Bordenave, S., Nouet, J., et al. (2010). Skeletal growth, ultrastructure and composition of the azooxanthellate scleractinian coral *Balanophyllia regia*. *Coral Reefs* 29, 175–189. doi: 10.1007/s00338-009-0557-x
- Bryan, W. H., and Hill, D. (1941). Spherulitic crystallization as a mechanism of skeletal growth in the hexacorals. *Proc. Royal Soc. Qld.* 52, 78–91.
- Buster, N.A., and Holmes, C.W. (2006). Magnesium content within the skeletal architecture of the coral *Montastraea faveolata*: locations of brucite precipitation and implications to fine-scale data fluctuations. *Coral Reefs* 25, 243–253. doi: 10.1007/s00338-006-0092-y
- Cuif, J.P., and Dauphin, Y. (1998). Microstructural and physico-chemical characterization of 'centers of calcification' in septa of some recent scleractinian corals. *Paläontologische Zeitschrift* 72, 257–269.
- Cuif, J.P., and Dauphin, Y. (2005). The two-step mode of growth in the scleractinian coral skeletons from the micrometre to the overall scale. *J. Struct. Biol.* 150, 319–331. doi: 10.1016/j.jsb.2005.03.004
- Cuif, J.P., Dauphin, Y., Doucet, J., Salome, M., and Susini, J. (2003). XANES mapping of organic sulfate in three scleractinian coral skeletons. *Geochim. Cosmochim. Acta* 67, 75–83. doi: 10.1016/S0016-7037(02)01041-4
- Domart-Coulon, I., Stolarski, J., Brahmi, C., Gutner-Hoch, E., Janiszewska, K., Shemesh, A., et al. (2014). Simultaneous extension of both basic microstructural components in scleractinian coral skeleton during night and daytime, visualized by *in situ* 86sr pulse labeling. *J. Struct. Biol.* 185, 79–88. doi: 10.1016/j.jsb.2013.10.012
- Frankowiak, K., Kret, S., Mazur, M., Meibom, A., Kitahara, M.V., and Stolarski, J. (2016). Fine-scale skeletal banding can distinguish symbiotic from asymbiotic species among modern and fossil scleractinian corals. *PLoS ONE* 11:e0147066. doi: 10.1371/journal.pone.0147066

- Gagnon, A.C., Adkins, J.F., Fernandez, D.P., and Robinson, L.F. (2007). Sr/Ca and Mg/Ca vital effects correlated with skeletal architecture in a scleractinian deep-sea coral and the role of Rayleigh fractionation. *Earth Planet. Sci. Lett.* 261, 280–295. doi: 10.1016/j.epsl.2007.07.013
- Giri, S.J., Swart, P.K., and Devlin, Q.B. (2017). The effect of changing seawater Ca and Mg concentrations upon the distribution coefficients of Mg and Sr in the skeletons of the scleractinian coral *Pocillopora damicornis*. *Geochim. Cosmochim. Acta* 222, 535–549. doi: 10.1016/j.gca.2017.11.011
- Gutner-Hoch, E., Schneider, K., Stolarski, J., Domart-Coulon, I., Yam, R., Meibom, A., et al. (2016). Evidence for rhythmicity pacemaker in the calcification process of scleractinian coral. *Sci. Rep.* 6:20191. doi: 10.1038/srep20191
- Higuchi, T., Fujimura, H., Yuyama, I., Harii, S., Agostini, S., and Oomori, T. (2014). Biotic control of skeletal growth by scleractinian corals in aragonite–calcite seas. *PLoS ONE* 9:e91021. doi: 10.1371/journal.pone.0091021
- Holcomb, M., Cohen, A.L., Gabbitov, R.I., and Hutter, J.L. (2009). Compositional and morphological features of aragonite precipitated experimentally from seawater and biogenically by corals. *Geochim. Cosmochim. Acta* 73, 4166–4179. doi: 10.1016/j.gca.2009.04.015
- Kramarsky-Winter, E., Downs, C. A., Downs, A., and Loya, Y. (2009). Cellular responses in the coral *Stylophora pistillata* exposed to eutrophication from fish mariculture. *Evol. Ecol. Res.* 11, 381–401.
- Kvitt, H., Kramarsky-Winter, E., Maor-Landaw, K., Zandbank, K., Kushmaro, A., Rosenfeld, H., et al. (2015). Breakdown of coral colonial form under reduced pH conditions is initiated in polyps and mediated through apoptosis. *Proc. Nat. Acad. Sci. U.S.A.* 112, 2082–2086. doi: 10.1073/pnas.1419621112
- Leclerc, J. A., Reynaud, S., Dissard, D., Tisserand, G., and Ferrier-Pagès, C. (2014). Light is an active contributor to the vital effects of coral skeleton proxies. *Geochim. Cosmochim. Acta* 140, 671–690. doi: 10.1016/j.gca.2014.05.042
- Mass, T., Drake, J.L., Haramaty, L., Kim, J.D., Zelzion, E., Bhattacharya, D., et al. (2013). Cloning and characterization of four novel coral acid-rich proteins that precipitate carbonates *in vitro*. *Curr. Biol.* 23, 1126–1131. doi: 10.1016/j.cub.2013.05.007
- Mass, T., Giuffrè, A.J., Sun, C.Y., Stiffler, C.A., Frazier, M.J., Neder, M., et al. (2017). Amorphous calcium carbonate particles form coral skeletons. *Proc. Nat. Acad. Sci.* 114, E7670–E7678. doi: 10.1073/pnas.1707890114
- Meibom, A., Cuif, J.P., Hillion, F., Constantz, B.R., Juillet-Leclerc, A., Dauphin, Y., et al. (2004). Distribution of magnesium in coral skeleton. *Geophys. Res. Lett.* 31:L23306. doi: 10.1029/2004GL021313
- Meibom, A., Yurimoto, H., Cuif, J. P., Domart-Coulon, I., Houlbrequé, F., Constantz, B., et al. (2006). Vital effects in coral skeletal composition display strict three-dimensional control. *Geophys. Res. Lett.* 33:L025968. doi: 10.1029/2006GL025968
- Meibom, A., Cuif, J.P., Houlbrequé, F., Mostefaoui, S., Dauphin, Y., Meibom, K.L., et al. (2008). Compositional variations at ultra-structure length scales in coral skeleton. *Geochim. Cosmochim. Acta* 72, 1555–1569. doi: 10.1016/j.gca.2008.01.009
- Meibom, A., Mostefaoui, S., Cuif, J.P., Dauphin, Y., Houlbrequé, F., Dunbar, R., et al. (2007). Biological forcing controls the chemistry of reef-building coral skeleton. *Geophys. Res. Lett.* 34:L02601. doi: 10.1029/2006GL028657
- Muscantine, L., Tambutte, E., and Allemand, D. (1997). Morphology of coral desmocytes, cells that anchor the calcoblastic epithelium to the skeleton. *Coral Reefs* 16, 205–213.
- Nodthdruff, L.D., Webb, G.E., Buster, N.A., Holmes, C.W., and Sorauf, J.E. (2005). Brucite microbialites in living coral skeletons: indicators of extreme microenvironments in shallow-marine settings. *Geology* 33, 169–172. doi: 10.1130/G20932.1
- Raz-Bahat, M., Erez, J., and Rinkevich, B. (2006). *In vivo* light-microscopic documentation for primary calcification processes in the hermatypic coral *Stylophora pistillata*. *Cell Tissue Res.* 325, 361–368. doi: 10.1007/s00441-006-0182-8
- Reynaud, S., Ferrier-Pages, C., Meibom, A., Mostefaoui, S., Mortlock, R., Fairbanks, R., et al. (2007). Light and temperature effects on Sr/Ca and Mg/Ca ratios in the scleractinian coral *Acropora* sp. *Geochim. Cosmochim. Acta* 71, 354–362. doi: 10.1016/j.gca.2006.09.009
- Shapiro, O.H., Kramarsky-Winter, E., Gavish, A.R., Stocker, R., and Vardi, A. (2016). A coral-on-a-chip microfluidic platform enabling live-imaging microscopy of reef-building corals. *Nat. Commun.* 7:10860. doi: 10.1038/ncomms10860
- Stolarski, J. (2003). Three-dimensional micro- and nanostructural characteristics of the scleractinian coral skeleton: a biocalcification proxy. *Acta Palaeontol. Pol.* 48, 497–530.
- Venn, A. A., Tambutté, E., Holcomb, M., Laurent, J., Allemand, D., and Tambutté, S. (2013). Impact of seawater acidification on pH at the tissue–skeleton interface and calcification in reef corals. *Proc. Natl. Acad. Sci. U.S.A.* 110, 1634–1639. doi: 10.1073/pnas.1216153110
- Venn, A., Tambutté, E., Holcomb, M., Allemand, D., and Tambutté, S. (2011). Live tissue imaging shows reef corals elevate pH under their calcifying tissue relative to seawater. *PLoS ONE* 6:e20013. doi: 10.1371/journal.pone.0020013
- Von Euw, S., Zhang, Q., Manichev, V., Murali, N., Gross, J., Feldman, L.C., et al. (2017). Biological control of aragonite formation in stony corals. *Science* 356, 933–938. doi: 10.1126/science.aam6371

Conflict of Interest Statement: The authors declare that the research was conducted in the absence of any commercial or financial relationships that could be construed as a potential conflict of interest.

Copyright © 2018 Shapiro, Kartvelishvily, Kramarsky-Winter and Vardi. This is an open-access article distributed under the terms of the Creative Commons Attribution License (CC BY). The use, distribution or reproduction in other forums is permitted, provided the original author(s) and the copyright owner(s) are credited and that the original publication in this journal is cited, in accordance with accepted academic practice. No use, distribution or reproduction is permitted which does not comply with these terms.